



ARTICLE

Biocomposites of Polylactic Acid Reinforced by DL-Lactic Acid-Grafted Microfibrillated Cellulose

Chaodong Liu, Yutong Yang, Boyu Cui and Weihong Wang*

Key Laboratory of Bio-Based Material Science and Technology (Ministry of Education), Material Science and Engineering College, Northeast Forestry University, Harbin, 150040, China

*Corresponding Author: Weihong Wang. Email: weihongwang2001@nefu.edu.cn

Received: 13 October 2021 Accepted: 03 December 2021

ABSTRACT

Microfibrillated cellulose (MFC) is often added to polylactic acid (PLA) matrixes as a reinforcing filler to obtain fully-biodegradable composites with improved mechanical properties. However, the incompatibility between MFC and the PLA matrix limits the mechanical performance of MFC-reinforced PLA composites. In this paper, DL-lactic acid-grafted-MFC (MFC-g-DL) was used to improve the compatibility with PLA. Reinforced composites were prepared by melt extrusion and hot-cold pressing. The tensile strength of the PLA/MFC-g-DL composite increased by 22.1% compared with that of PLA after adding 1% MFC-g-DL. Scanning electron microscopy (SEM), differential scanning calorimetry (DSC), and dynamic thermomechanical analysis (DMA) were used to explore the enhancement mechanism. The energy dissipation in the MFC network and the improved compatibility between PLA and MFC-g-DL played important roles in the reinforcement. The SEM results showed that there was a closer combination between PLA and MFC-g-DL. The DSC results showed that the addition of cellulose changed the glass transition temperature, melting temperature, and crystallization temperature of PLA. The TG results showed that the initial and maximum decomposition temperature were lower than those of PLA. The ultraviolet spectra showed that the composite had good transparency at a low concentration of MFC-g-DL.

KEYWORDS

Polylactic acid; microfibrillated cellulose; tensile properties; transparency

1 Introduction

Cellulose is a renewable, degradable, and biocompatible material that can be easily obtained from wood, crop straw, and many other plants [1]. After the physical or chemical treatment of cellulose, four different products with a high specific strength and high modulus can be obtained: cellulose nanocrystals (CNC), cellulose nanofibers (CNF), microcrystalline cellulose (MCC), and microfibrillated cellulose (MFC) [2,3]. Many studies have shown that composites with better mechanical properties can be obtained by adding cellulose [4–8]. Among these kinds of cellulose fibers, MFC retains both crystalline and non-crystalline regions. Compared with CNF, MFC requires a lower energy consumption during its preparation. Compared with MCC, MFC is more environmentally friendly and does not require acid treatment [9,10]. A series of composites containing MFC have been obtained [11–14].



The shortage of petroleum resources and serious pollution caused by non-degradable petroleum-based plastics have promoted the applications of biodegradable materials. As a completely biodegradable plastic, polylactic acid (PLA) has been vigorously developed [15]. The preparation of cellulose-reinforced PLA composites also has attracted extensive attention, but there are crucial problems to solve to obtain composites with better performance [16]. Firstly, hydroxyl groups on the surface of cellulose lead to its aggregation in polymer matrixes and also give it a high polarity, which leads to poor compatibility with non-polar polymers; therefore, the number of hydroxyl groups in cellulose must be reduced. Chemical modification is an often-used method with remarkable effects [17–21]. Lee et al. [22] converted the hydrophilic groups on CNCs into alkyl groups via nucleophilic substitution with alkyl bromide. The alkylated CNCs-reinforced PLA nanocomposites had good thermal stability, tensile strength, Young's modulus, and barrier properties due to the better dispersion and higher hydrophobicity of CNCs in non-polar environments. Jamaluddin et al. [23] prepared an acetylated PLA/CNF composite with good transparency and improved mechanical properties without reducing the thermal stability of PLA.

To toughen brittle polylactic acid (PLA) composites, Qian et al. [24] modified bamboo cellulose nanowhiskers (BCNW) with (3-mercaptopropyl) trimethoxysilane and then combined them with a PLA matrix. The elongation at break of the PLA/BCNW composite was 250.8%, while it was only 12.35% for the untreated composite. Surface modification can reduce cellulose aggregation and promote the uniform dispersion of cellulose in polymer matrixes [25,26]. Although chemical modification methods have achieved good results, the modification processes often involve many reaction steps and produce environmental pollution [27]. In addition, after the chemical treatment of cellulose, the composites are often prepared by solvent casting [22–24,28–33], but this method is unfavorable to the environment and difficult to expand its production.

Another difficulty is induced by moisture contained within cellulose. PLA is sensitive to moisture, so it must be removed because wet cellulose tends to severely agglomerate during oven drying. Some special drying methods, such as freeze-drying, spray-drying, and supercritical CO₂ drying have been used to remove moisture [34–36], but these methods are often expensive and difficult to industrialize. The efficient drying of nanocellulose at a low cost to reduce agglomeration remains a major challenge that restricts the use of cellulose in composites. Moreover, the addition of cellulose can improve some properties of PLA, but it may negatively impact other properties. Therefore, how to reduce these negative impacts is an urgent problem to solve [24,37–40].

In this study, a new method was developed to reduce the agglomeration of MFC in a PLA matrix and improve their interfacial compatibility. MFC was grafted with DL-lactic acid monomer, oven-dried at 60°C, and then mixed with PLA. PLA/MFC-*g*-DL composites were prepared by hot-cold pressing. Both the mechanical and thermal properties of the cellulose-reinforced PLA composites were significantly improved by this green and facile method, and the high transparency of PLA was maintained.

2 Experimental

2.1 Materials

The polylactic acid (PLA, 2003 D, D-lactic acid: 1.4%, L-lactic acid: 98.6%, granular, density 1.24 g/cm³, melt index 5.0–7.0 g/10 min) had a number average and weight average molecular weight of ~150,000 Da and ~200,000 Da, respectively, and was provided by Nature Works (USA). Microfibrillated cellulose (MFC), with 75% water content, was produced by Saigelu Chemical Industry Company, Japan. DL-Lactic acid (analytically pure), 85%–90%, 90.08 (weight-average molecular weight) was supplied by Macklin of China. Zinc acetate (analytically pure) was purchased from Aladdin of China.

2.2 Modification of MFC with DL-Lactic Acid

Before the grafting reaction, an MFC suspension with a concentration of 1% was prepared and treated using an ultrasonic cell crusher (Scientz-18 N, power: 800 W, Ningbo, China) for 30 min. Then, 200 ml MFC

suspension, 100 g DL-lactic acid, and 0.1 g zinc acetate were successively added to a flask. The flask was assembled into a distillation unit, and the oil bath temperature was set to 170°C. Upon increasing the temperature, the water in the MFC suspension was continuously discharged. After about 200 ml of distilled water was collected, the reaction was continued for 20 min and then cooled to room temperature. The product was washed with deionized water and filtered three times to remove unreacted DL-lactic acid. The collected product was further prepared into a suspension with a concentration of 1% and named MFC-g-DL. The MFC-g-DL suspension was placed in a glass Petri dish and dried in an electrothermal blow-drying box at 60°C, and then processed into powder by a pulverizer.

2.3 Preparation of Cellulose-Reinforced PLA Composite Film

Before preparing the composite, PLA was dried in an electrothermal blow-drying box for 12 h at 60°C. MFC-g-DL powder and PLA were melted and compounded in a conical twin-screw micro-extruder (JZSZ-10A Wuhan, Wuhan Ruiming Experimental Instrument Manufacturing Co., Ltd., China). The PLA/MFC-g-DL mixture was hot-pressed for 3 min at 180°C under 0.1 MPa and then 5 min at the same temperature under 5 MPa pressure, and then cooled to room temperature. The film with dimensions of 10 cm × 10 cm × 0.4 mm was obtained. The proportion of MFC-g-DL and MFC in the composite film was 0.5%, 1%, 2%, 3%, and 4%, respectively. Using the same preparation method, a PLA film was prepared as a control sample.

3 Characterization Methods

3.1 Fourier-Transform Infrared Spectroscopy

The chemical properties of MFC were analyzed by a Fourier-transform infrared spectrometer (FTIR, Nicolet 6700, Thermo Fisher Scientific Instruments Co., USA). The scanning range was 400 to 4000 cm⁻¹.

3.2 Tensile Property Test

The tensile properties of PLA and its composites were analyzed by a universal testing machine (CMT-5504, Shenzhen Xinsansi Material Testing Co., China) according to the reference standard GB/T 1040.2-2006 (Determination of plastic tensile properties).

3.3 Differential Scanning Calorimetry

The crystallization behavior of PLA and its composites was analyzed by differential scanning calorimetry (DSC, Q20, TA Company, USA). The samples were first heated from 30°C to 200°C at a rate of 10 °C/min and then held at 200°C for 5 min. Then, the temperature was rapidly lowered to 30°C and held for 5 min. The samples were then re-heated to 200°C at a speed of 10 °C/min.

3.4 Thermogravimetric Analysis

The thermal stability of PLA and its composites were analyzed by a thermogravimetric analyzer (Q50, TA Company, USA). The test temperature range was 30°C–450°C, and the heating speed was 10 °C/min.

3.5 Dynamic Thermomechanical Analysis

The thermomechanical properties of PLA and its composites were analyzed by a dynamic thermomechanical analyzer (DMA, Q800, TA Company, USA). The sample dimensions were 30 mm × 10 mm × 0.4 mm. The test temperature range was 25°C–120°C, the heating speed was 3 °C/min, the frequency was 1 Hz, and the amplitude was 15 μm.

3.6 Transmittance Test

The transmittance of PLA and its composites was measured by a UV-visible spectrophotometer (Cary100, Agilent, USA). The scanning wavelength range was 190–900 nm with an interval of 1 nm.

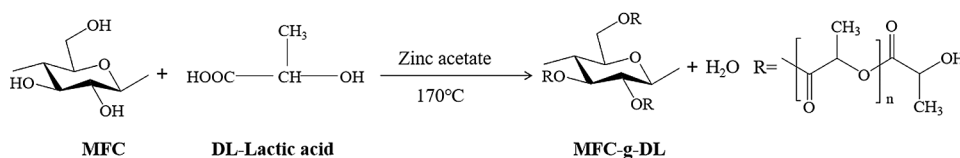
3.7 Microstructure Observation by Scanning Electron Microscopy

The samples of PLA and its composites were first gold-sprayed in a vacuum-coating machine and then scanning electron microscopy (SEM, EM-30 Plus, Korea Coolsham Company, Korea) was used to observe their surface and tensile cross-sections. The accelerating voltage was 10 kV.

4 Results and Discussion

4.1 Characteristics of MFC and DL-Lactic Acid-Modified MFC

Scheme 1 shows the molecular model for the chemical reaction of the MFC-grafted DL-lactic acid monomer. The esterification reaction started after gradually removing water from the mixture of the MFC suspension and lactic acid. Then, lactic acid units were grafted onto the surface of MFC. Fig. 1 shows the infrared spectra of ungrafted and grafted MFC (MFC-g-DL). A new absorption peak appeared in the spectrum of MFC-g-DL at 1740 cm^{-1} , which corresponded to $-\text{COO}^-$, which was not observed in the ungrafted MFC. This indicated that the esterification reaction between MFC and DL-lactic acid occurred.



Scheme 1: DL-Lactic acid-modified MFC

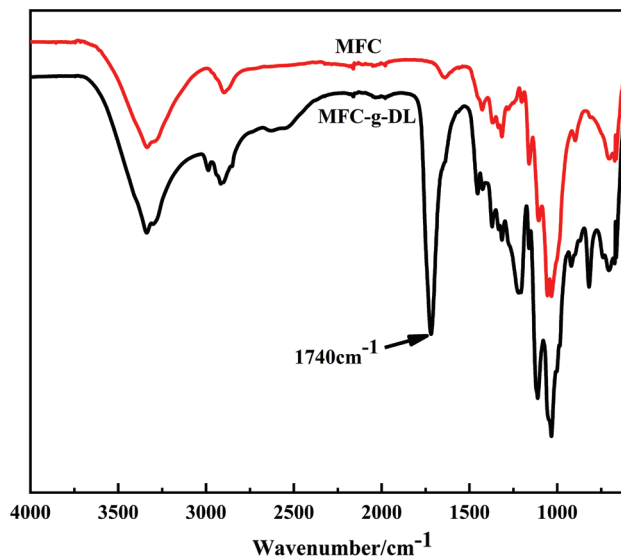


Figure 1: FTIR spectra of MFC-g-DL and MFC

4.2 Tensile Properties of PLA and Its Composites

Fig. 2a shows that the tensile properties of PLA were improved by introducing MFC-g-DL at a suitable amount. When 0.5% and 1% MFC-g-DL were added, the tensile strength of PLA MFC-g-DL composites increased by 23% and 22.1%. The enhancement of MFC-g-DL was much greater than that of MFC because of the improved compatibility between MFC-g-DL and PLA. However, as the concentration increased, this strengthening gradually weakened due to the uneven distribution of excessive cellulose in the PLA matrix. Agglomeration occurred and caused stress concentration in the composite. The same trend was

observed in the tensile modulus (Fig. 2b). Fig. 2c shows that both MFC-g-DL and MFC decreased the elongation at break of the composite, which is similar to previous results in the literature [39,40].

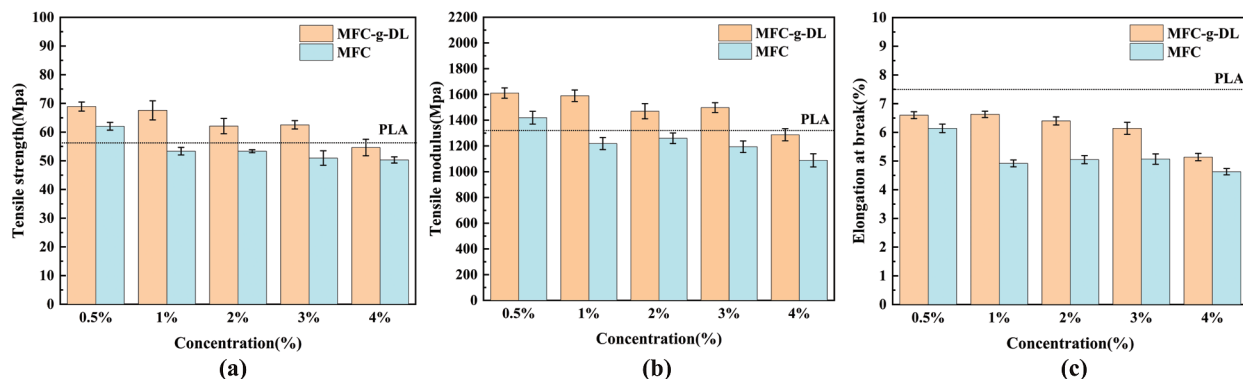


Figure 2: Tensile properties of PLA and its composites: (a) Tensile strength, (b) tensile modulus, and (c) elongation at break

Grafted cellulose was more easily dispersed in the PLA matrix; therefore, the composite could accommodate more cellulose. A significant decrease in tensile properties occurred at 2% MFC-g-DL, however, 1% for MFC. Overall, when the concentration of MFC-g-DL was set at 0.5% and 1%, the PLA/MFC-g-DL composites showed improved tensile strength and modulus.

4.3 DSC Analysis

Fig. 3 shows the DSC results of PLA and its composites. The glass transition temperature (T_g), cold crystallization temperature (T_{cc}), melting temperature (T_{m1} , T_{m2}), cold crystallization enthalpy (ΔH_{cc}), and melting enthalpy (ΔH_m) obtained from DSC are summarized in Table 1. The crystallinities of PLA and its composites were calculated as follows:

$$\chi_{sample}\% = (\Delta H_m - \Delta H_{CC}) / \Delta H_m^0 \times 100\% \tag{1}$$

where ΔH_m^0 is the melting enthalpy of 100% crystalline PLA (93.1 J/g).

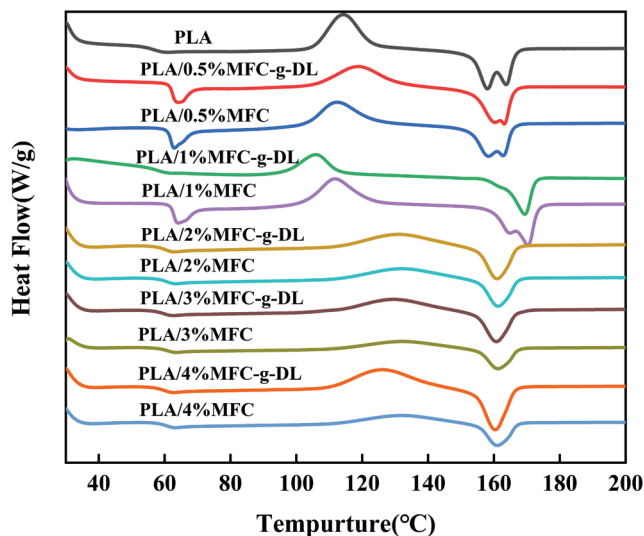


Figure 3: DSC curves of PLA and its composites

The DSC results are summarized in Table 1.

Table 1: DSC results of PLA and its composites

Sample	T_g (°C)	T_{cc} (°C)	T_{m1} (°C)	T_{m2} (°C)	ΔH_{cc} (J/g)	ΔH_m (J/g)	X (%)
PLA	60.09	117.43	158.40	163.68	34.98	38.48	3.8
PLA/0.5%MFC-g-DL	64.06	118.68	161.21	163.42	29.38	37.48	8.7
PLA/0.5%MFC	62.67	112.15	158.48	162.99	31.79	37.17	5.8
PLA/1%MFC-g-DL	61.31	105.99	169.511	–	26.62	35.90	9.9
PLA/1%MFC	64.17	111.75	164.93	170.37	32.19	36.97	5.1
PLA/2%MFC-g-DL	61.23	129.30	161.04	–	31.35	33.79	2.6
PLA/2%MFC	62.81	131.51	161.39	–	16.0	20.24	4.6
PLA/3%MFC-g-DL	62.43	129.30	161.04	–	17.23	19.45	2.4
PLA/3%MFC	62.17	132.06	161.28	–	21.78	23.55	1.9
PLA/4%MFC-g-DL	61.55	125.77	160.49	–	23.62	29.01	5.8
PLA/4%MFC	62.89	132.06	161.28	–	30.7	32.92	2.4

Compared with pure PLA, the T_g of all PLA/cellulose composites increased slightly because the addition of cellulose may have hindered the segmental flexibility of PLA chains [41]. The T_{cc} of PLA/cellulose composites was lower than that of PLA, indicating that cellulose promoted the crystallization of PLA at lower cellulose concentrations [42]. Double melting is common in many semi-crystalline polymers. The main mechanisms are (i) the presence of more than one crystallographic form; (ii) the presence of crystalline lamellar populations characterized by different thicknesses or perfection; (iii) simultaneous melting and recrystallization [43]. The T_{m1} and T_{m2} of the PLA composites were higher than that of PLA, except for PLA/0.5% MFC. This indicated that the reinforcement by grafted MFC or a sufficient amount of ungrafted MFC improved the thermal stability of PLA. The addition of cellulose improved the crystallinity of PLA to varying degrees at a low concentration. This observation suggests that MFC acted as a nucleating agent for PLA and promoted the crystallization of PLA. This phenomenon is consistent with the conclusions reached in most literatures [44–46]. The role of MFC-g-DL was significantly greater than that of MFC. The decreased crystallinity and the higher T_{cc} of the composites may have been caused by the higher cellulose concentration, which limited the mobility of PLA molecular chains [47,48].

4.4 TGA and DTG Analysis

The TGA and DTG curves of pure PLA and its composites are shown in Fig. 4. The initial decomposition temperature (T_{onset}), maximum decomposition temperature (T_{max}), and Mass loss obtained from TG are summarized in Table 2. The T_{onset} and T_{max} of PLA were 308°C and 358°C, respectively. Compared with PLA, these two temperatures of the cellulose-reinforced composites were lower due to the addition of cellulose because the initial decomposition temperature of cellulose was about 250°C–300°C [27]. MFC-g-DL and MFC-reinforced PLA composites showed similar degradation temperatures, which indicated that grafting did not change the thermal decomposition behavior of MFC.

4.5 DMA Analysis

Fig. 5a shows the effect of the cellulose concentration on the storage modulus of PLA. The storage modulus of PLA was about 5000 MPa, which decreased after reaching the glass transition temperature. The addition of MFC and MFC-g-DL to the PLA matrix increased the storage modulus considerably, indicating that cellulose acted as an efficient reinforcement in the polymer [49]. When 0.5% MFC was

added, the storage modulus increased by more than 10%, and MFC-g-DL resulted in a greater increase (nearly 20%) than MFC. This was consistent with the tensile strength and tensile modulus results and was due to the better interfacial compatibility between MFC-g-DL and the PLA matrix.

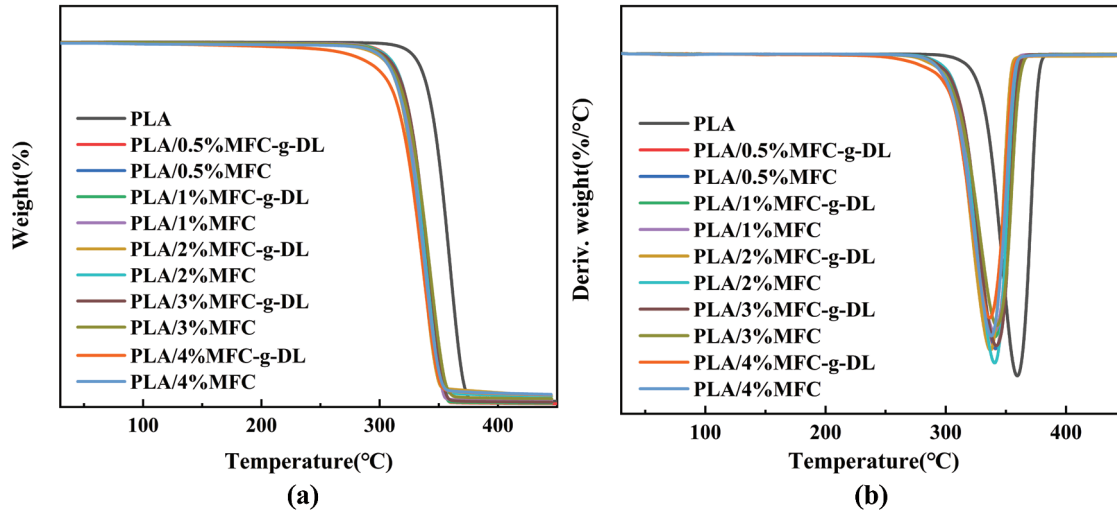


Figure 4: Thermal stability of PLA and its composites: (a) TGA curve and (b) DTG curve

Table 2: Thermal stability analysis of PLA and its composites

Sample	T_{onset} (°C)	T_{max} (°C)	Mass loss (%)
PLA	308.21	358.75	98.41
PLA/0.5%MFC-g-DL	292.64	338.98	98.35
PLA/0.5%MFC	291.71	338.45	98.56
PLA/1%MFC-g-DL	290.21	339.12	97.93
PLA/1%MFC	290.25	337.98	97.98
PLA/2%MFC-g-DL	289.41	338.52	97.85
PLA/2%MFC	288.51	338.49	98.56
PLA/3%MFC-g-DL	287.45	337.79	98.95
PLA/3%MFC	287.01	337.96	98.76
PLA/4%MFC-g-DL	254.68	334.52	97.88
PLA/4%MFC	278.41	338.48	98.64

The $\tan\delta$ curves (Fig. 5b) show that due to the addition of cellulose, the composite presented a sharper and more intense peak than PLA. This indicated that the loss modulus of cellulose-reinforced PLA had a larger viscoelastic proportion in the composites than PLA. Thus, the composites obtained in this work did not present a large decrease in toughness, unlike other composites reported in the literature [44].

4.6 Transparency Analysis

The UV spectra showed that PLA had good transparency. When 0.5% and 1% MFC-g-DL were added, there was no obvious effect on the transparency of PLA (Fig. 6a). Fig. 6a also shows that when these two films with different MFC-g-DL concentrations were used to cover the school's emblem, the school

emblem was still visible. However, MFC reduced the transparency from 100% to 75% and 70% at concentrations of 0.5% and 1%, respectively, likely due to MFC agglomeration and the loose interface with the matrix [50].

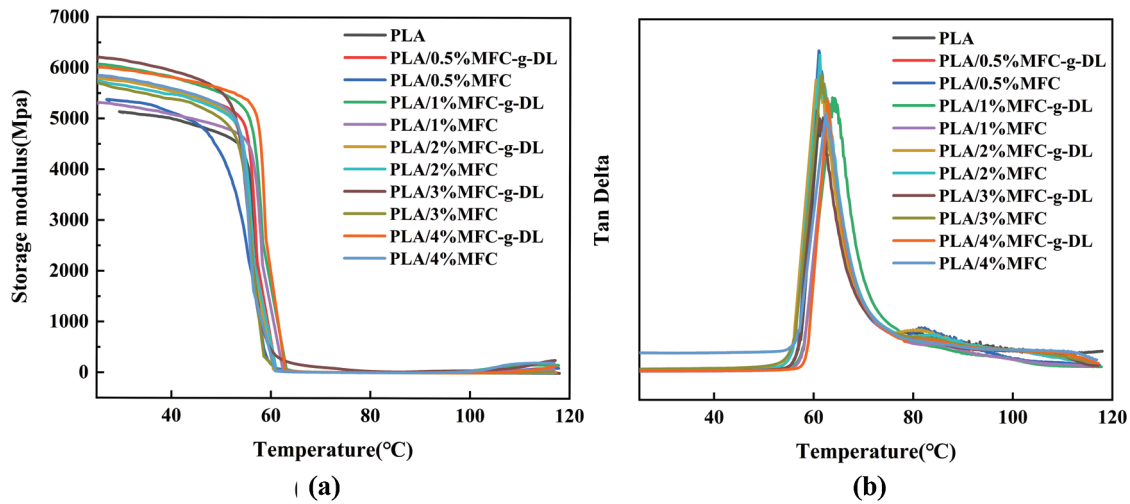


Figure 5: Dynamic mechanical analysis of PLA and its composites: (a) Storage modulus and (b) $\tan\delta$

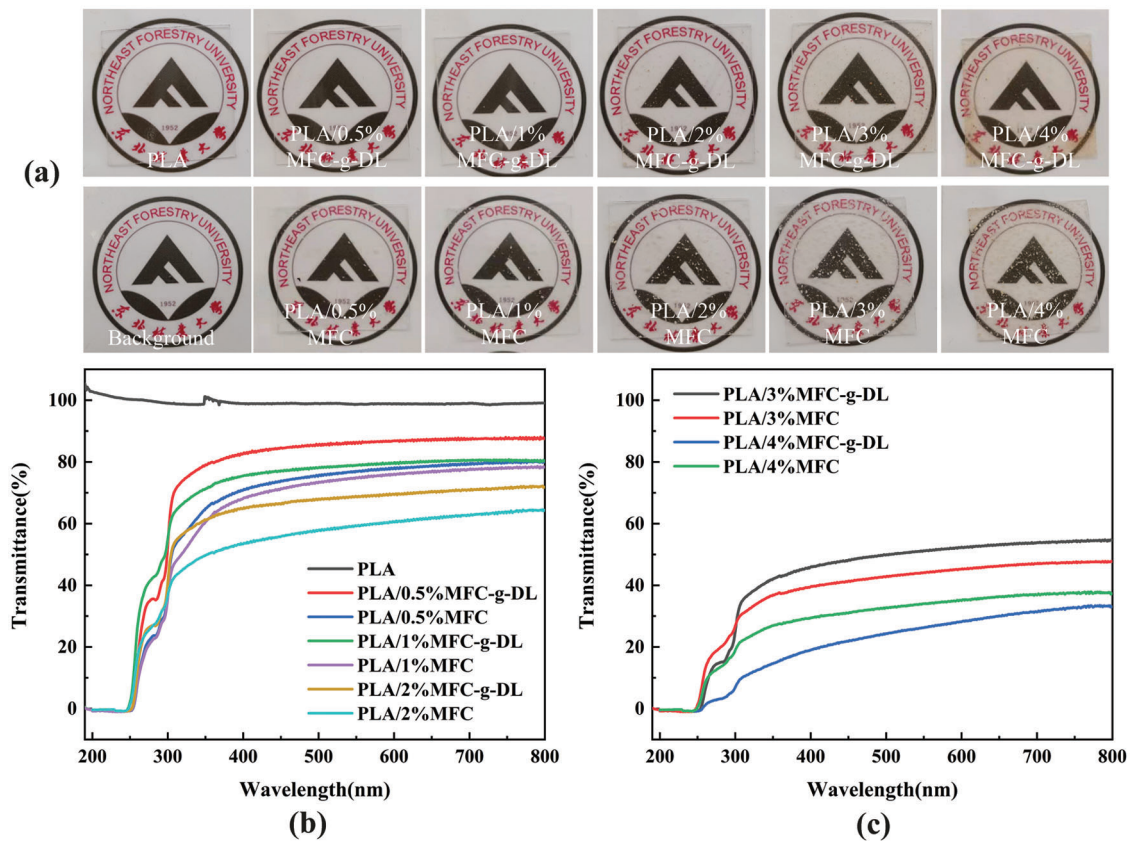


Figure 6: (a) Digital images of the composite placed over the school emblem, and (b) (c) UV spectra

4.7 Microstructure of PLA Composites

Interfacial compatibility is one of the most important factors determining the properties of composites. MFC-g-DL provided the composite with higher tensile properties than MFC. As expected, the better interfacial bonding between MFC-g-DL and the PLA matrix was observed in Fig. 7. These results showed that modifying MFC with DL-lactic acid improved its interfacial compatibility with PLA, so as to obtain cellulose-reinforced PLA composites. However, higher concentrations of cellulose no longer enhanced the tensile strength of PLA, which was mainly caused by the agglomeration of cellulose in PLA.

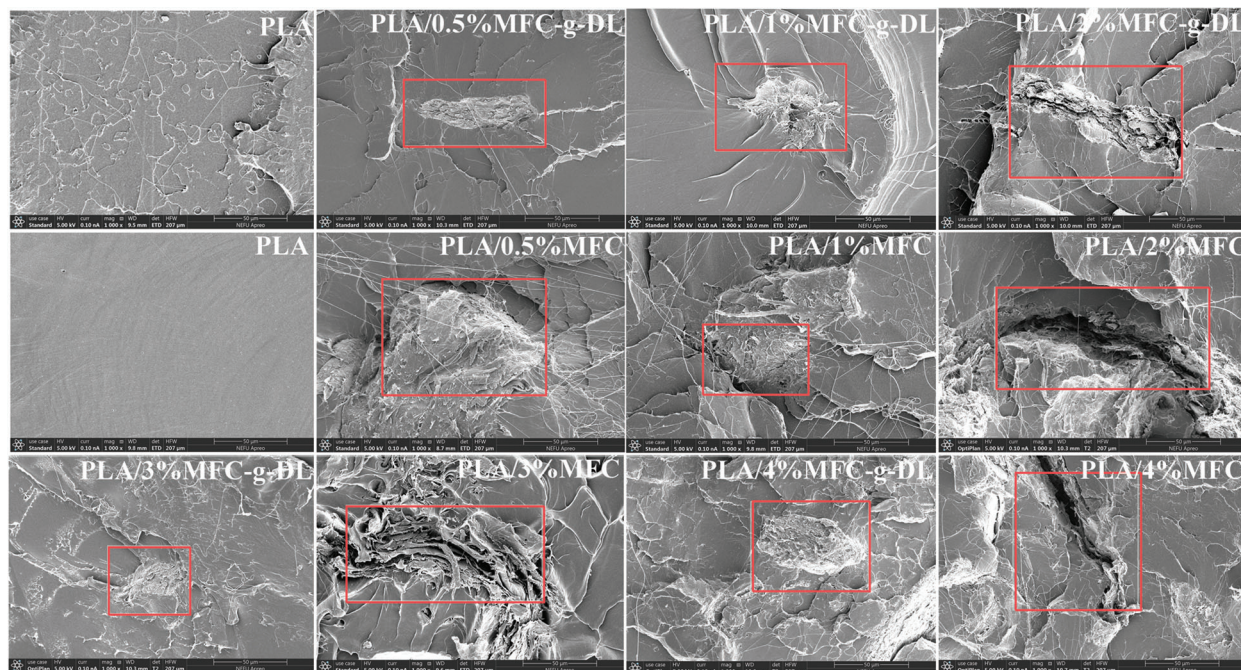


Figure 7: SEM images of PLA and its composites

5 Conclusions

In this study, DL-lactic acid monomer was introduced to modify MFC to improve its compatibility with a PLA matrix. Reinforced composites were obtained by melt extrusion and hot-cold pressing. Due to the presence of MFC-g-DL, the tensile strength and tensile modulus of PLA were improved. The addition of cellulose promoted PLA crystallization and improved its thermal stability. The light transmittance of the PLA/MFC-g-DL composite film was better than that of the PLA/MFC composite film at the same concentration. This method is environmentally friendly and has a facile procedure.

Funding Statement: This research was supported by the Natural Science Foundation of China (No. 32071704).

Conflicts of Interest: The authors declare that they have no conflicts of interest to report regarding the present study.

References

1. Li, T., Chen, C., Brozena, A. H., Zhu, J. Y., Xu, L. et al. (2021). Developing fibrillated cellulose as a sustainable technological material. *Nature*, 590(7844), 47–56. DOI 10.1038/s41586-020-03167-7.

2. Lamm, M. E., Li, K., Qian, J., Wang, L., Lavoine, N. et al. (2021). Recent Advances in functional materials through cellulose nanofiber templating. *Advanced Materials*, 33(12), 2005538. DOI 10.1002/adma.202005538.
3. Li, K., Skolrood, L. N., Aytug, T., Tekinalp, H., Ozcan, S. (2019). Strong and tough cellulose nanofibrils composite films: Mechanism of synergetic effect of hydrogen bonds and ionic interactions. *ACS Sustainable Chemistry & Engineering*, 7(17), 14341–14346. DOI 10.1021/acssuschemeng.9b03442.
4. Li, J., Jiang, Z., Qiu, Z. (2021). Thermal and rheological properties of fully biodegradable Poly (ethylene succinate)/Cellulose nanocrystals composites. *Composites Communications*, 23, 100571. DOI 10.1016/j.coco.2020.100571.
5. Silva, C. G., Campini, P. A. L., Rocha, D. B., Rosa, D. S. (2019). The influence of treated eucalyptus microfibers on the properties of PLA biocomposites. *Composites Science and Technology*, 179, 54–62. DOI 10.1016/j.compscitech.2019.04.010.
6. Hendren, K. D., Baughman, T. W., Deck, P. A., Foster, E. J. (2020). *In situ* dispersion and polymerization of polyethylene cellulose nanocrystal-based nanocomposites. *Journal of Applied Polymer Science*, 137(13), 48500. DOI 10.1002/app.48500.
7. Maia, T. H. S., Larocca, N. M., Beatrice, C. A. G., de Menezes, A. J., de Freitas Siqueira, G. et al. (2017). Polyethylene cellulose nanofibrils nanocomposites. *Carbohydrate Polymers*, 173, 50–56. DOI 10.1016/j.carbpol.2017.05.089.
8. Ryu, Y. S., Lee, J. H., Kim, S. H. (2020). Efficacy of alkyl ketene dimer modified microcrystalline cellulose in polypropylene matrix. *Polymer*, 196, 122463. DOI 10.1016/j.polymer.2020.122463.
9. Ng, H. K. M., Leo, C. P. (2019). Translucent and adsorptive PVA thin film containing microfibrillated cellulose intercalated with TiO₂ nanoparticles for dye removal. *Colloids and Surfaces A: Physicochemical and Engineering Aspects*, 578, 123590. DOI 10.1016/j.colsurfa.2019.123590.
10. Vu, C. M., Nguyen, D. D., Sinh, L. H., Choi, H. J., Pham, T. D. (2017). Micro-fibril cellulose as a filler for glass fiber reinforced unsaturated polyester composites: Fabrication and mechanical characteristics. *Macromolecular Research*, 26(1), 54–60. DOI 10.1007/s13233-018-6006-3.
11. Palange, C., Johns, M. A., Scurr, D. J., Phipps, J. S., Eichhorn, S. J. (2019). The effect of the dispersion of microfibrillated cellulose on the mechanical properties of melt-compounded polypropylene-polyethylene copolymer. *Cellulose*, 26(18), 9645–9659. DOI 10.1007/s10570-019-02756-8.
12. Kim, S. H., Kim, E. S., Choi, K., Cho, J. K., Sun, H. et al. (2018). Rheological and mechanical properties of polypropylene composites containing microfibrillated cellulose (MFC) with improved compatibility through surface silylation. *Cellulose*, 26(2), 1085–1097. DOI 10.1007/s10570-018-2122-7.
13. Kargazadeh, H., Mariano, M., Huang, J., Lin, N., Ahmad, I. et al. (2017). Recent developments on nanocellulose reinforced polymer nanocomposites: A review. *Polymer*, 132, 368–393. DOI 10.1016/j.polymer.2017.09.043.
14. Wang, G., Yang, X., Wang, W. (2019). Reinforcing linear low-density polyethylene with surfactant-treated microfibrillated cellulose. *Polymers (Basel)*, 11(3), 441. DOI 10.3390/polym11030441.
15. Kalita, N. K., Sarmah, A., Bhasney, S. M., Kalamdhad, A., Katiyar, V. (2021). Demonstrating an ideal compostable plastic using biodegradability kinetics of poly (lactic acid) (PLA) based green biocomposite films under aerobic composting conditions. *Environmental Challenges*, 3, 100030. DOI 10.1016/j.envc.2021.100030.
16. Rai, P., Mehrotra, S., Priya, S., Gnansounou, E., Sharma, S. K. (2021). Recent advances in the sustainable design and applications of biodegradable polymers. *Bioresource Technology*, 325(6510), 124739. DOI 10.1016/j.biortech.2021.124739.
17. Li, K., Wang, Y., Rowe, M., Zhao, X., Li, T. et al. (2019). Poly (lactic acid) toughening through chain end engineering. *ACS Applied Polymer Materials*, 2(2), 411–417. DOI 10.1021/acscpm.9b00888.
18. Salmén, L., Stevanic, J. S. (2018). Effect of drying conditions on cellulose microfibril aggregation and hornification. *Cellulose*, 25(11), 6333–6344. DOI 10.1007/s10570-018-2039-1.
19. Sinquefield, S., Ciesielski, P. N., Li, K., Gardner, D. J., Ozcan, S. (2020). Nanocellulose dewatering and drying: Current state and future perspectives. *ACS Sustainable Chemistry & Engineering*, 8(26), 9601–9615. DOI 10.1021/acssuschemeng.0c01797.

20. Bharadwaz, A., Jayasuriya, A. C. (2020). Recent trends in the application of widely used natural and synthetic polymer nanocomposites in bone tissue regeneration. *Materials Science & Engineering C, Materials for Biological Applications*, 110(5), 110698. DOI 10.1016/j.msec.2020.110698.
21. Yin, Y., Zhao, L., Jiang, X., Wang, H., Gao, W. (2018). Cellulose nanocrystals modified with a triazine derivative and their reinforcement of poly (lactic acid)-based bionanocomposites. *Cellulose*, 25(5), 2965–2976. DOI 10.1007/s10570-018-1741-3.
22. Lee, J. H., Park, S. H., Kim, S. H. (2020). Surface alkylation of cellulose nanocrystals to enhance their compatibility with polylactide. *Polymers*, 12(1), 178. DOI 10.3390/polym12010178.
23. Jamaluddin, N., Kanno, T., Asoh, T. A., Uyama, H. (2019). Surface modification of cellulose nanofiber using acid anhydride for poly (lactic acid) reinforcement. *Materials Today Communications*, 21, 100587. DOI 10.1016/j.mtcomm.2019.100587.
24. Qian, S., Sheng, K. (2017). PLA toughened by bamboo cellulose nanowhiskers: Role of silane compatibilization on the PLA bionanocomposite properties. *Composites Science and Technology*, 148(8), 59–69. DOI 10.1016/j.compscitech.2017.05.020.
25. Ogunsona, E. O., Panchal, P., Mekonnen, T. H. (2019). Surface grafting of acrylonitrile butadiene rubber onto cellulose nanocrystals for nanocomposite applications. *Composites Science and Technology*, 184, 107884. DOI 10.1016/j.compscitech.2019.107884.
26. Arslan, D., Vatansever, E., Sarul, D. S., Kahraman, Y., Gunes, G. et al. (2020). Effect of preparation method on the properties of polylactide/cellulose nanocrystal nanocomposites. *Polymer Composites*, 41(10), 4170–4180. DOI 10.1002/pc.25701.
27. Li, K., McGrady, D., Zhao, X., Ker, D., Tekinalp, H. et al. (2021). Surface-modified and oven-dried microfibrillated cellulose reinforced biocomposites: Cellulose network enabled high performance. *Carbohydrate Polymers*, 256(1), 117525. DOI 10.1016/j.carbpol.2020.117525.
28. Wu, H., Nagarajan, S., Shu, J., Zhang, T., Zhou, L. et al. (2018). Green and facile surface modification of cellulose nanocrystal as the route to produce poly (lactic acid) nanocomposites with improved properties. *Carbohydrate Polymers*, 197(2), 204–214. DOI 10.1016/j.carbpol.2018.05.087.
29. Takkalkar, P., Tobin, M. J., Vongsvivut, J., Mukherjee, T., Nizamuddin, S. et al. (2019). Structural, thermal, rheological and optical properties of poly (lactic acid) films prepared through solvent casting and melt processing techniques. *Journal of the Taiwan Institute of Chemical Engineers*, 104(10–11), 293–300. DOI 10.1016/j.jtice.2019.08.018.
30. Shojaeiarani, J., Bajwa, D. S., Stark, N. M. (2018). Spin-coating: A new approach for improving dispersion of cellulose nanocrystals and mechanical properties of poly (lactic acid) composites. *Carbohydrate Polymers*, 190(4), 139–147. DOI 10.1016/j.carbpol.2018.02.069.
31. Trifol, J., van Drongelen, M., Clegg, F., Plackett, D., Szabo, P. et al. (2019). Impact of thermal processing or solvent casting upon crystallization of PLA nanocellulose and/or nanoclay composites. *Journal of Applied Polymer Science*, 101, 47486. DOI 10.1002/app.47486.
32. Rigotti, D., Pegoretti, A., Miotello, A., Checchetto, R. (2020). Interfaces in biopolymer nanocomposites: Their role in the gas barrier properties and kinetics of residual solvent desorption. *Applied Surface Science*, 507, 145066. DOI 10.1016/j.apsusc.2019.145066.
33. Sarul, D. S., Arslan, D., Vatansever, E., Kahraman, Y., Durmus, A. et al. (2021). Preparation and characterization of PLA/PBAT/CNC blend nanocomposites. *Colloid and Polymer Science*, 299(6), 987–998. DOI 10.1007/s00396-021-04822-9.
34. Góis, G. S., Nepomuceno, N. C., França, C. H. A., Almeida, Y. M. B., Hernández, E. P. et al. (2018). Influence of morphology and dispersion stability of CNC modified with ethylene oxide derivatives on mechanical properties of PLA-based nanocomposites. *Polymer Composites*, 40(S1), 399–408. DOI 10.1002/pc.
35. Abdallah, W., Mirzadeh, A., Tan, V., Kamal, M. R. (2018). Influence of nanoparticle pretreatment on the thermal, rheological and mechanical properties of PLA-PBSA nanocomposites incorporating cellulose nanocrystals or montmorillonite. *Nanomaterials*, 9(1), 29. DOI 10.3390/nano9010029.

36. Matsuyama, K., Morotomi, K., Inoue, S., Nakashima, M., Nakashima, H. et al. (2019). Antibacterial and antifungal properties of Ag nanoparticle-loaded cellulose nanofiber aerogels prepared by supercritical CO₂ drying. *The Journal of Supercritical Fluids*, 143, 1–7. DOI 10.1016/j.supflu.2018.08.008.
37. Li, L., Chen, Y., Yu, T., Wang, N., Wang, C. et al. (2019). Preparation of polylactic acid/TEMPO-oxidized bacterial cellulose nanocomposites for 3D printing via Pickering emulsion approach. *Composites Communications*, 16, 162–167. DOI 10.1016/j.coco.2019.10.004.
38. Patwa, R., Saha, N., Saha, P., Katiyar, V. (2019). Biocomposites of poly (lactic acid) and lactic acid oligomer-grafted bacterial cellulose: It's preparation and characterization. *Journal of Applied Polymer Science*, 136(35), 47903. DOI 10.1002/app.47903.
39. Zhang, Q., Lei, H., Cai, H., Han, X., Lin, X. et al. (2020). Improvement on the properties of microcrystalline cellulose/polylactic acid composites by using activated biochar. *Journal of Cleaner Production*, 252, 119889. DOI 10.1016/j.jclepro.2019.119898.
40. He, L., Song, F., Li, D. F., Zhao, X., Wang, X. L. et al. (2020). Strong and tough polylactic acid based composites enabled by simultaneous reinforcement and interfacial compatibilization of microfibrillated cellulose. *ACS Sustainable Chemistry & Engineering*, 8(3), 1573–1582. DOI 10.1021/acssuschemeng.9b06308.
41. Boruvka, M., Behalek, L., Lenfeld, P., Brdlik, P., Habr, J. et al. (2020). Solid and microcellular polylactide nucleated with PLA stereocomplex and cellulose nanocrystals. *Journal of Thermal Analysis and Calorimetry*, 142(2), 695–713. DOI 10.1007/s10973-020-09477-2.
42. Wang, Q., Ji, C., Sun, J., Zhu, Q., Liu, J. (2020). Structure and properties of polylactic acid biocomposite films reinforced with cellulose nanofibrils. *Molecules*, 25(14), 3306. DOI 10.3390/molecules25143306.
43. Frone, A. N., Panaitescu, D. M., Chiulan, I., Nicolae, C. A., Vuluga, Z. et al. (2016). The effect of cellulose nanofibers on the crystallinity and nanostructure of poly (lactic acid) composites. *Journal of Materials Science*, 51(21), 9771–9791. DOI 10.1007/s10853-016-0212-1.
44. Du, Y., Wu, T., Yan, N., Kortschot, M. T., Farnood, R. (2014). Fabrication and characterization of fully biodegradable natural fiber-reinforced poly (lactic acid) composites. *Composites Part B: Engineering*, 56(4), 717–723. DOI 10.1016/j.compositesb.2013.09.012.
45. Lee, H. J., Ryu, Y. S., Kim, I. S., Kim, S. H. (2019). Pretreatment of microfibrillated cellulose on polylactide composites. *Macromolecular Research*, 28(2), 110–117. DOI 10.1007/s13233-020-8016-1.
46. Vanhatalo, K., Lundin, T., Koskimäki, A., Lillandt, M., Dahl, O. (2016). Microcrystalline cellulose property-structure effects in high-pressure fluidization: microfibril characteristics. *Journal of Materials Science*, 51(12), 6019–6034. DOI 10.1007/s10853-016-9907-6.
47. Xu, C., Lv, Q., Wu, D., Wang, Z. (2017). Polylactide/cellulose nanocrystal composites: A comparative study on cold and melt crystallization. *Cellulose*, 24(5), 2163–2175. DOI 10.1007/s10570-017-1233-x.
48. Sung, S. H., Chang, Y., Han, J. (2017). Development of polylactic acid nanocomposite films reinforced with cellulose nanocrystals derived from coffee silverskin. *Carbohydrate Polymers*, 169, 495–503. DOI 10.1016/j.carbpol.2017.04.037.
49. Zhang, Y., Cui, L., Xu, H., Feng, X., Wang, B. et al. (2019). Poly (lactic acid)/cellulose nanocrystal composites via the Pickering emulsion approach: Rheological, thermal and mechanical properties. *International Journal of Biological Macromolecules*, 137(1), 197–204. DOI 10.1016/j.ijbiomac.2019.06.204.
50. Jamaluddin, N., Hsu, Y. I., Asoh, T. A., Uyama, H. (2021). Effects of acid-anhydride-modified cellulose nanofiber on poly (Lactic Acid) composite films. *Nanomaterials*, 11(3), 753. DOI 10.3390/nano11030753.